THE ASTROPHYSICAL JOURNAL, 178:1–24, 1972 November 15

THE REDSHIFT-DISTANCE RELATION. II. THE HUBBLE DIAGRAM AND ITS SCATTER FOR FIRST-RANKED CLUSTER GALAXIES: A FORMAL VALUE FOR q_0

ALLAN SANDAGE
Hale Observatories, Carnegie Institution of Washington, California Institute of Technology
Received 1972 May 8

ABSTRACT

The Hubble diagram for first-ranked cluster galaxies is discussed on the basis of new photoelectric measurements of 41 clusters. Additional data by Westerlund and Wall and by Peterson, reduced by the same corrections, increase the sample to 84 clusters.

The diagram has small scatter about a line of slope 5. Analysis of the scatter gives upper limits to the dispersions in redshift and in apparent magnitude, respectively. Treated as redshift residuals, the data show $\Delta \log z$ to be independent of z; and because of this, most of the scatter must be due to residuals in magnitude. A limit of $\sigma(\Delta cz) \simeq 100$ km s^{-1} for the distribution of random velocities of cluster centers in the present sample can be put from the analysis.

From the magnitude residuals, the dispersion in absolute luminosities of first-ranked galaxies is $\sigma(\Delta M_V) = 0.25$ mag. For such galaxies in the present sample, the absolute magnitudes are independent of richness of the parent cluster over a richness range $5 \lesssim N \lesssim 500$.

There is no evidence for intergalactic absorption for galaxies in the present sample, either patchy at the $\sigma = 0.25$ mag level, or general and selective at the $\sigma[E(B - V)] \simeq 0.05$ mag level.

If a strictly homogeneous Friedmann model universe is adopted, the deceleration parameter is calculated to be $q_0 = 0.96 \pm \sim 0.4$ (p.e.). To reduce this formal value to $q_0 = 0$ requires a luminosity evolution at the rate $dM/dt = 1.09\,(1 + z)H_0$ mag yr^{-1}, in the sense that E galaxies were brighter in the past.

With $q_0 = +1$ and $H_0 = 50$ km s^{-1} Mpc^{-1}, the time to the Friedmann singularity is 11×10^9 years, which agrees with the age of globular clusters in our own Galaxy.

I. INTRODUCTION

Hubble (1929) discovered the velocity-distance relation by correlating redshifts and apparent magnitudes of nearby galaxies. This correlation (herein called the Hubble diagram) had been previously suggested by Robertson (1928) but was not discussed in detail by him. The diagram has been the format for discussions of the expansion of the Universe to progressively larger redshifts (Humason 1931; Hubble and Humason 1931; Humason 1936; Hubble 1936, 1953; Humason, Mayall, and Sandage 1956 [hereafter called HMS]; Sandage 1968*c*) from 1930 to the present.

If enough redshift and magnitude data were available for a class of galaxies that have a small dispersion in absolute magnitude, the information could be used to map the kinematic and dynamic properties of the expansion in detail. These properties include the basic kinematic flow, its second-order modifications described as shear and rotation of the actual Universe, and the dynamical effect of deceleration caused by self-gravity.

A general method of finding the second-order flow components has been developed by Kristian and Sachs (1966), who made no assumption that the Universe is homogeneous and isotropic. Data for galaxies in many directions and at many distances are required to carry out such a program in detail, and sufficient data do not now exist.

Although it is known that the actual Universe is close to the homogeneous model in some of its local properties (i.e., the flow is $cz \simeq Hr$ to good approximation and the expansion is closely isotropic), there is no guarantee that real departures from homogeneity and isotropy have no effect on the determination of the deceleration parameter q_0. Until proof is available that the large-scale shear and rotation are, in fact, smaller than certain critical values, any current determination of q_0 must rest on the postulate that the actual Universe does not deviate significantly from a homogeneous model. There are reasons to expect that in the next several years enough data will be obtained to permit a realistic solution. As a start, some of these questions will be discussed in a subsequent paper of this series where an exploratory test of the validity of the Friedmann solution is given using the presently available data.

But the problem of adequately mapping the velocity field is more basic than merely the question of the choice of model because such mapping cannot be done *at any level* unless certain conditions are met. (1) Are the apparent magnitudes of the galaxies chosen as distance indicators related to some distance parameter in a well enough defined way so that the derived flow is not badly distorted by mapping errors? The answer requires knowledge of the absolute magnitude of test galaxies and of the evolutionary change of their luminosity with time. (2) Are the measured redshifts related to the expansion motion uniquely? To what extent do virial velocities and other extraneous effects mask the expansion effect? (3) Is space sufficiently transparent to permit apparent magnitudes of even ideal probes to be uniquely (monotonically) related to distance; and if so, is *any* correction for intergalactic absorption needed?

A study of the scatter in the Hubble diagram gives limits on (1) any noncosmological redshift component Δz, (2) the dispersion in absolute magnitude of the test galaxies, and (3) the amount of patchy intergalactic absorption. The data show that the first-ranked cluster galaxies are sufficiently homogeneous in absolute luminosity that very low limits can be put on items (1) and (3). The limits are sufficiently small that cosmological information can be obtained either by the method of Kristian and Sachs or by model fitting. This need not have been the case, but the remarkable homogeneity of first-ranked cluster elliptical galaxies (a fact that is surely important in understanding at least part of their physics) clears away many technical obstacles that would otherwise be present in a search for cosmological effects in this way.

This paper is concerned primarily with the nature of the scatter in the Hubble diagram and with the conclusions concerning the galaxies themselves that can be drawn therefrom.

New photometric data for cluster galaxies are listed and discussed in § II; the correlations leading to the Hubble diagram in § III; other data by Westerlund and Wall and by Peterson in § IV; the resulting Hubble diagram in § V; analysis of the scatter leading to limits on noncosmological redshift components Δz, to the dispersion of first-ranked cluster galaxies, and to the transparency of space in § VI; limits on a correlation between absolute luminosity of first-ranked cluster galaxies and cluster richness in § VII; and a solution for q_0 using a Friedmann model in § VIII.

II. NEW PHOTOMETRY OF HMS CLUSTERS AND TEN 3CR RADIO SOURCES

A photometric program on clusters of galaxies was begun in 1963 because of the heterogeneity of the magnitudes for the galaxies discussed by HMS (their tables 12 and 13), and because no magnitudes of any kind existed for many of the 26 clusters for which Humason had measured redshifts (HMS tables 2 and 3).

Magnitudes in B and V were measured for most clusters of known redshift using 1P21 photomultipliers and the 60-, 100-, and 200-inch (152-, 254-, and 508-cm) reflectors at Mount Wilson and Palomar during parts of six observing seasons. Pulse-counting methods were used with equipment built by the Astroelectronics Laboratory.

TABLE 1

PHOTOELECTRIC DATA FOR BRIGHT MEMBERS OF CLUSTERS OF GALAXIES

CLUSTER	z	Tel	Aperture	V	B	B-V	REMARKS
Virgo	0.00378	60 Hol	Total	8.49	9.44	0.96	Brightest E in
NGC 4472	or	De Vauc	Total	8.4	9.4	1.0	core of Virgo
	0.00316			8.45	9.42		Cluster.
Fornax	0.00519	100P	202	9.14	10.05	0.91	Brightest E in
NGC 1316	or	Sersic	Total	8.9	9.9	1.0	Fornax Cl. M03-31
	0.00478						
Peg I	0.01279	100P	25.0	12.54	13.58	1.04	
2317+0755		60P	68.9	11.95	13.04	1.09	
		100P	80.5	11.72	12.74	1.02	NGC 7619
		60P	136.1	11.36	12.37	1.00	
		100P	202	11.29	12.33	1.04	
		100P	25.0	12.60	13.63	1.03	
		60P	68.9	11.98	13.01	1.03	
		100P	80.5	12.02	12.95	0.93	NGC 7626
		60P	136.1	11.61	12.63	1.02	
		100P	144.4	11.57	12.61	1.04	
		100P	202	11.28	12.30	1.02	
0122+3305	0.0170	100S	35.2	12.80	13.83	1.03	NGC 507
			64.0	12.36	13.42	1.06	
Perseus	0.01811	60S	24.6	12.91	13.63	0.72	
NGC 1275			24.6	12.96	13.66	0.70	
			41.6	12.53	13.29	0.76	
			41.6	12.58	13.31	0.73	
			69.2	12.18	12.99	0.81	
			69.2	12.28	13.03	0.75	
Coma	0.0222	200S	12.2	13.62	14.69	1.07	
NGC 4889		200S	18.8	13.19	14.25	1.06	
		200S	30.6	12.80	13.86	1.06	
		100P	40.6	12.67	13.73	1.06	
		200S	48.3	12.46	13.51	1.05	
		60P	68.8	12.01	13.07	1.06	
		60P	136	11.62	12.68	1.06	
Hercules	0.0347	60P	42.3	14.00	14.90	0.90	
		60P	68.9	13.81	14.73	0.92	IC1185
		100P	40.6	14.53	15.66	1.13	IC1183
		60P	42.3	14.56	15.49	0.93	
		60P	68.9	14.22	15.27	1.05	IC1194
2308+0720	0.0428	60P	68.9	13.93	14.97	1.04	NGC 7503 of Peg II
		100P	80.5	13.44	14.55	1.11	
2322+1425	0.0439	100S	35.2	14.49	15.58	1.09	N8 of HMS
NGC 7649							
1145+5559	0.0516	200S	18.8	15.01	16.13	1.12	
UMa #1			30.6	14.74	15.88	1.14	N24 of HMS
			48.3	14.58	15.69	1.11	
			18.8	15.11	16.22	1.11	
			18.8	15.10	16.22	1.12	
			30.6	14.82	15.95	1.13	N7 of HMS
			48.3	14.60	15.71	1.11	
			18.8	15.45	16.53	1.08	
			30.6	15.25	16.31	1.06	N25 of HMS
			18.8	15.79	16.74	0.95	N15: SBO galaxy
			30.6	15.70	16.65	0.95	14mm E, 4mm S of
							N24 on HMS chart
0106-1536	0.0526	100S	35.2	14.05	15.07	1.02	
Haufen A		100P	40.6	13.74	14.92	1.18	N1+N2 of HMS
		100S	64.0	13.47	14.56	1.09	of HMS chart
		100S	64.0	13.67	14.59	0.92	Δmag=0.60
		100S	35.2	14.98	16.05	1.07	N4: E2 galaxy
							5mm W, 2mm S of
							N2 on HMS chart
		100S	35.2	15.06	15.78	0.72	N3: E6 galaxy
							1mm E, 3mm S of
							N2 on HMS chart
1024+1039	0.0649	200S	12.2	15.61	16.85	1.24	N1: North and
Leo			18.8	15.36	16.53	1.17	West of N2.
			30.6	15.12	16.27	1.15	
			12.2	16.01	17.16	1.15	N2: South and
			18.8	15.74	16.92	1.18	East of N1.
			30.6	15.60	16.76	1.16	

CLUSTER	z	Tel	Aperture	V	B	B-V	REMARKS
1239+1852	0.0718	200S	18.8	15.06	16.27	1.21	N4 of HMS
Virgo 2			30.6	14.74	15.92	1.18	
			12.2	15.50	16.68	1.18	N2: E2 galaxy 6mm W, 13mm S
			18.8	15.25	16.44	1.19	of N4 on HMS chart.
			30.6	15.07	16.27	1.20	
1520+2754	0.0722	200S	18.8	15.76	16.96	1.20	
Cor Bor			30.6	15.52	16.69	1.17	N2 of HMS.
			48.3	15.34	16.55	1.21	
			30.6	15.58	16.76	1.18	N6 of HMS.
			30.6	15.96	17.17	1.21	N3 of HMS.
			48.3	15.95	17.10	1.15	
0705+3506	0.0779	200S	12.2	16.02	17.28	1.26	N1 of HMS.
			18.8	15.48	16.69	1.21	18#8 contaminated.
			12.2	16.22	17.47	1.25	
			18.8	15.95	17.18	1.23	N2 of HMS
			30.6	15.78	17.09	1.31	
1513+0433	0.0944	200S	18.8	15.93	17.20	1.27	
			30.6	15.72	16.91	1.19	N1 of HMS.
			18.8	16.12	17.38	1.26	N2: 3mm E, 5mm S of
			30.6	15.92	17.20	1.28	N1 on HMS chart.
			18.8	16.46	17.73	1.27	N3: 10mm E, 8mm S of
			30.6	16.35	17.57	1.22	N1 on HMS.
1431+3146	0.1312	200S	12.2	16.66	18.02	1.36	
Bootis			18.8	16.34	17.61	1.27	N1 of HMS.
			12.2	16.71	18.15	1.44	N9: 5mm W, 28mm N of
			18.8	16.40	.....	.....	N1 of HMS. Off HMS
			18.8	16.21	17.67	1.46	chart.
			30.6	16.20	.....	.....	
			12.2	17.73	19.24	1.51	N4 of HMS.
			18.8	(17.79	19.05	1.26)	18#8 suspect.
			30.6	14.03	14.62	0.59	NGC 5672, U-B=-0.09.
							Foreground
1055+5702	0.1345	200S	7.6	17.37	18.32	0.95	N1 of HMS.
UMa #2			7.6	17.39	19.11	1.72	N2 of HMS.
			18.8	16.35	17.65	1.30	N1+N2 of HMS.
N1 is a			30.6	16.25	17.42	1.17	N1+N2 of HMS.
supergiant							
by appearance			12.2	17.26	18.68	1.42	N3 of HMS.
on plates.							
			12.2	16.96	18.43	1.47	N5: 7mm W, 2mm S of N3
			18.8	16.58	18.16	1.58	on HMS chart
			12.2	16.49	17.93	1.44	N10: 28mm E, 34mm S
			18.8	16.29	17.64	1.35	of N3 on HMS chart.
1153+2341	0.1426	200S	18.8	15.93	17.39	1.46	N1+N1A of HMS.
			30.6	15.53	16.93	1.40	Δmag = 1.8
			12.2	17.67	(19.36)	(1.69)	N2: 0.5mm W, 3mm S of
			18.8	17.52	18.96	1.44	of N1 on HMS chart.
			12.2	17.78	19.16	1.38	N4: 12mm W, 13mm N
			18.8	17.89	19.38	1.49	of N1 on HMS chart.
1534+3749	0.1532	200S	12.2	17.26	18.70	1.44	N1 of HMS.
			18.8	16.97	18.46	1.49	Contaminated by Star
			30.6	16.73	18.12	1.39	at 30.6?
			12.2	17.48	18.89	1.41	N2: 3mm W, 3mm S of
			18.8	17.31	18.73	1.42	N1 on HMS chart.
			18.8	17.30	18.73	1.43	
			30.6	17.23	18.66	1.43	
			18.8	17.56	18.94	1.38	N4: 1mm W, 27mm S of
							N1 on HMS chart.
			30.6	17.03	18.45	1.42	N6: 28mm W, 3mm N of
							N1: off HMS chart.
			12.2	13.20	14.23	1.03	Star 11mm W, 6mm S of N1
							on HMS chart. U-B=0.73.

(*continued*)

TABLE 1 -continued

CLUSTER	z	Tel	Aperture	V	B	B-V	REMARKS
0025+2223	0.1594	200S	12.2	17.22	18.70	1.48	N4 of HMS
			18.8	17.03	18.54	1.51	
			12.2	17.60	19.14	1.54	N2: 16mm W, 9mm N of
			18.8	17.43	18.92	1.49	N4 on HMS chart.
			12.2	17.83	19.37	1.54	N1: 19mm W, 20mm S
			18.8	17.71	19.13	1.42	of N4: off HMS chart
1228+1050	0.1651	200S	7.6	17.65	19.20	1.55	N1 of HMS.
Virgo 3			7.6	17.99	19.54	1.55	N2 of HMS.
			18.8	16.67	18.20	1.53	N1+N2.
			30.6	16.50	(17.90)	(1.40)	N1+N2.
			12.2	17.78	19.34	1.56	N4: 13mm E, 13mm S
			18.8	17.60	19.12	1.52	of N2 on HMS chart
0138+1832	0.1730	200S	12.2	18.04	19.51	1.47	N1 of HMS.
			18.8	17.71	19.25	1.54	
			12.2?	18.46	20.04	1.58	ND: 12mm W, 15mm S
							of N1: off HMS chart
			12.2	18.97	20.03	1.06	NA: 9mm E, 4mm S of
							N1 on HMS chart
1309-0105	0.1745	200S	12.2	17.55	18.97	1.42	N3: 5mm E, 5mm N of
			18.8	17.28	18.64	1.36	N2 on HMS chart
			12.2	17.08		1.48	N1+N2 in HMS
1304+3110	0.1831	200S	12.2	17.50	19.08	1.58	N1+N1A+N1B on
			18.8	16.87	18.52	1.65	HMS chart. Δmag=0.9
N1A+N1B			12.2	17.92	19.44	1.52	N3: 18mm W, 9mm S
combined light			18.8	17.81	19.23	1.42	of N1.
is 0.3 mag							
fainter than			12.2	18.26	19.80	1.54	N2: 7mm W, 7 mm S
N2			18.8	18.03	19.37	(1.34)	of N1.
0925+2044	0.1917	200S	12.2	17.10	18.79	1.69	N1+N1A of HMS
			18.8	16.99	18.64	1.65	Δmag≈3.
			12.2	17.78	19.42	1.64	N10: 32mm W, 10mm S
							of N1. Off HMS chart
			12.2	17.87	19.40	1.53	N2: 3mm E, 4mm S of
			18.8	17.60	19.29	1.69	N1 on HMS chart

ADDENDUM 1971

CLUSTER	z	Tel	Aperture	V	B	B-V	ϵ_V	ϵ_B
1641+1327	0.1499	200S	18″8	17.13	18.71	1.58	±0.011	±0.026
1447+2617	0.36							
N4		200S	12.2	19.93	21.42	1.49	±0.078	±0.220
N3		200S	12.2	20.17	21.38	1.21	±0.092	±0.142
0024+1654	0.38	200 Oke	7	19.85	.....	....	.....	.....
3C295	0.461	200S	7.6	19.76	21.22	1.46	±0.048	±0.102
N1*			12.2	19.56	20.94	1.38	±0.093	±0.147
N2			7.6	20.94	.....	....	±0.099	.....

CLUSTER	z	Tel	Aperture	V	B	B-V	REMARKS
1253+4422	0.1979	200S	12.2	18.32	(19.68)	(1.36)	N1: 24mm W, 9mm N
			12.2	18.20	(20.00)	(1.80)	of N2 on HMS chart.
			12.2	18.87	20.48	1.61	N3: 30mm W, 9 mm N
							of N2.
			12.2	18.91	20.52	1.61	N5: 19mm W, 14mm S
			12.2	18.70	20.16	1.46	of N2
			12.2	18.68	20.09	1.41	N8: 8mm E, 23mm N
							of N2 on HMS chart
			12.2	18.46	19.97	1.51	N9: 18mm E, 7 mm N of
							N2 on HMS chart
0855+0327	0.2018	200S	12.2	17.77	19.36	1.59	N1 of HMS
			18.8	17.70	19.29	1.59	
			12.2	17.20	18.70	1.50	N8 + N9 + N9A
			18.8	16.88	18.48	1.60	of HMS
			12.2	17.94	18.76	0.82	N10 of HMS
			12.2	18.24	19.82	1.58	N4: 1mm E, 3mm S of
							N1 on HMS chart
NGC 383	0.0169	60P	68.8	12.53	(13.71)	1.18:	HMS group, Table XI,
3C31							SO_3
NGC 545							
3C40	0.0180	100S	35.2	12.97	14.00	1.03	NGC 545 alone
Abell 194							
Δm_1=0.3			64.0	12.09	13.10	1.01?	NGC 545 +NGC 547
			112	11.85	12.89	1.04}	
			35.2	12.97	14.01	1.04	NGC 547 alone
3C66							
Near	0.0215	100S	20.0	13.86	14.94	1.08	N1
Abell			35.2	13.40	14.26	0.86	N1 plus star
347			11.2	14.81	15.71	0.90	Star alone
NGC 7720	0.0301	200S	12.2	14.43	15.59	1.16	N1
3C465			12.2	15.08	16.19	1.11	N2
Abell 2634			48.3	13.19	14.31	1.12	N1+N2
Δmag=0.7			72.4	12.94	14.03	1.09	N1+N2 N2 is in
							envelope of N1:
							Δmag=0.7
NGC 6166	0.0303	36Min	60	12.90	13.75	0.85	
3C338		+0'Dell	150	12.47	13.30	0.83	
Abell 2199							
3C317	0.0351	200S	30.6	14.06	15.13	1.07	Brightest of pair
Abell			48.3	13.62	14.63	1.06	
2052			30.6	14.72	15.74	1.02	Fainter of pair
M23-112	0.0825	200S	18.8	15.83	16.89	1.06	
Abell			30.6	15.52	16.49	0.97	
2638?			30.6	15.53	16.64	1.11	
3C219	0.1745	200S	12.2	17.49	18.99	1.50	Has companion
			18.8	17.10	18.67	1.57	18″8 may be contamins
3C28	0.1959	200S	12.2	17.87	19.37	1.50	
Abell			12.2	17.79	19.18	1.39	
115			18.8	17.62	18.95	1.33	
			18.8	17.47	18.92	1.45	

*N1 of 3C295 has 3 companions at Δ mag = 1.2, 1.3, and 1.7 fainter than N1. At aperture size of 7″6, the 1.2 and 1.3 mag galaxies contaminate the measurement. At size 12″2 all three contaminate. Correction gives V(7″6) = 20.30, V(12″2) = 20.18 which, with the standard aperture correction of Paper I gives V_{26} = 20.11 in the mean for N1 alone. Adopting a mean B-V = 1.42 gives B_{26} = 21.53.

Summaries of interim results have been published as they related to other problems (Sandage 1968*a*, *b*; Peach 1970), but the measurements, corrections, and final (m, z) pairs are only now given here.

Table 1 lists the observational data for 28 clusters whose redshifts were measured by Humason. Also listed is photometry for nine 3CR radio galaxies, all of which are themselves first-ranked members of clusters. Data for four very distant clusters are listed in the Addendum, as measured in 1971 after the bulk of table 1 was prepared.

The clusters in table 1 are arranged in order of redshift, listed in column (2). Column (3) gives the telescope and observer (P is Pettit 1954; H is Holmberg 1958; de Vaucouleurs 1961*a*, *b*; Sersic 1961; O'Dell for 3C 338 in Minkowski 1961; Oke 1971 for Cl 0024+1654; and S for Sandage here). Column (4) gives the diameter of the photoelectric aperture in arc seconds; columns (5), (6), and (7) give the photometry; and column (8) lists identification for the galaxy that was measured.

The mean redshift values in column (2) are mostly from Humason (HMS, tables 2 and 3). Exceptions are for the radio sources in the second part of the table where non–HMS attributions can be found in the notes to table 2 of Paper III (Sandage 1972*c*). For the four clusters in the Addendum, the redshift for 1641+1327 (Abell 2224) was supplied by Sargent; 3C 295 is by Minkowski (1960); and the two most distant clusters, 1447+2617 and 0024+1654, which Humason had studied with exceptional but unsuccessful tenacity (Bowen 1957), were measured by Baum (1962), and more recently by Oke (1971) using a variation of the color technique first proposed by Stebbins and Whitford (1948).

Two values are given for the mean redshifts of the Virgo and Fornax clusters. For Virgo, the HMS value of $\langle cz \rangle = 1136$ km s^{-1} is listed first, followed by de Vaucouleurs's (1961*b*) value of 950 km s^{-1} for the E cloud alone. Redshifts for five Fornax cluster members are listed in HMS, and an additional 10 are given by Mayall and de Vaucouleurs (1962). Averaging 18 available values for 15 galaxies, including the highly discordant case of NGC 1375 ($cz = -70$ km s^{-1}), gives $\langle cz \rangle = 1437$ km s^{-1}, or $\langle z \rangle = 0.0048$ for the Fornax cluster. Excluding NGC 1375 leaves 17 measurements of 14 different galaxies for a mean of $\langle cz \rangle = 1526$ km s^{-1}, or $\langle z \rangle = 0.0051$, which we adopt as the preferred value.

The identifications in the final column of table 1 are either NGC or IC numbers or refer to numbered galaxies on charts in HMS (plates 1 and 2) or to offsets therefrom.

The accuracy of the photometry has been judged both from the statistics of the photon counts, and from the internal consistency of repeated measurements in different seasons. The internal errors average $\epsilon_{V,B} \lesssim \pm 0.02$ mag (rms) for $V \lesssim 17$, and $\lesssim \pm 0.05$ mag per measurement fainter than $V \lesssim 18.5$. Formal internal errors, derived from the count-statistics, are listed in the addendum to table 1 for the faintest clusters.

Various corrections are required to these data before they can be used in a proper Hubble diagram.

III. CORRECTIONS TO THE MAGNITUDES

a) Aperture Corrections

Each measurement in table 1 was corrected for aperture effect by the precepts of Paper I (Sandage 1972*a*, table 3 and fig. 6). The arbitrary standard metric angular diameter is that of equation (23) of that paper. To define a proper metric diameter requires knowledge of q_0, and in the approximation adopted now, the growth curve of Paper I assumes $q_0 = +1$, an assumption that can, if necessary, be refined by a rapidly converging iteration (cf. Paper I).

The aperture correction has been made in two ways. (1) For galaxies with many data, it was sometimes possible to plot V_{meas} versus log $[\theta z/(1+z)^2]$, and to read V at 0.469 of the logarithmic variable. The method is internal and has been labeled I in column (9) of table 2. (2) In cases with insufficient data at large apertures, the standard curve in Paper I was applied to each measurement, giving values for the corrected magnitude, called hereafter V_{26} and B_{26}. These numbers, listed in table 2, are the mean of all such values for each galaxy. The symbol S for *standard curve* in column (9) of table 2 identifies this method.

The accuracy of the mean has been judged from the agreement of the many individual values, and is generally good, as the reader can verify by experimenting with table 1 and the growth curve of Paper I. Symbols for the quality of the fit are set out in table 2, column (9), where E denotes *excellent* when the deviation of the observations from the mean curve is less than ± 0.04 mag for either the I or S method. For quality G (good) the deviations are ± 0.07 mag; F (fair) has ± 0.10 mag, and P (poor) has $\sim \pm 0.15$ mag.

TABLE 2

PHOTOMETRIC PARAMETERS FOR FIRST RANKED GALAXIES IN 41 CLUSTERS (HMS + 3C RADIO)

Cluster (1)	Other (2)	Richness (3)	l^{II} (4)	b^{II} (5)	z (6)	V_{26} (7)	B_{26} (8)	Ap. Corr. (9)	Av (10)	A_B (11)	V_c (12)	B_c (13)	log CZ (14)	Remarks (15)
VIRGO	...	(1)	287	+70	0.00379*	8.45	9.42	Hol, T	0.00	0.00	8.45	9.42	3.056*	N4472
FORNAX	...	(1)	240	-57	0.00509*	8.90	9.90	Sersic, T	0.00	0.00	8.90	9.90	3.184*	N1316
PEG I	...	(0)	88	-48	0.0128	11.24	12.27	LS(E)	0.02	0.03	11.20	12.18	3.584	N7619
0122+3305	...	(1)	131	-29	0.0170	11.94	12.99	S(G)	0.22	0.29	11.70	12.62	3.710	N507
PERSEUS	A426	2	151	-13	0.0181	11.87	12.62	S(E)	0.30*	0.40*	11.54	12.13	3.735	N1275
COMA	A1656	2	57	+88	0.0222	(11.55)	(12.61)	De Vauc	0.00	0.00	(11.51)	(12.50)	3.824	N4889
HERCULES	A2151	2	32	+44	0.0341	13.22	14.14	I(E)	0.05	0.07	13.12	13.90	4.017	
2308+0720	PEGII	(0)	84	-48	0.0428	13.66	14.65	I,S(P)	0.02	0.03	13.57	14.40	4.109	N7503
2322+1425	A2589	0	93	-43	0.0440	14.21	15.30	S	0.06	0.09	14.08	14.99	4.120	N7649
1145+5559	A1377	1	141	+59	0.0516	14.47	15.59	I,S(E)	0.00	0.00	14.39	15.33	4.191	UMa#1
0106-1536	A151	1	143	-78	0.0526	14.12	15.17	I,S(F)	0.00	0.00	14.03	14.90	4.198	HaufA
1024+1039	A1020	1	233	+52	0.0649	14.92	16.11	I,S(E)	0.00	0.00	14.81	15.78	4.290	Leo
1239+1852	A1589	0	287	+81	0.0718	14.64	15.84	S(F)	0.00	0.00	14.52	15.48	4.333	Virgo#2
1520+2754	A2065	2	43	+57	0.0722	15.36	16.55	I(E)	0.00	0.00	15.24	16.18	4.334	Cor Bor
0705+3506	A568	0	182	+18	0.0779	15.46	16.71	I,S(E)	0.18*	0.24*	15.15	16.07	4.369	Gemini
1513+0433	A2048	1	5	+49	0.0944	15.66	16.84	I(E)	0.01	0.02	15.50	16.34	4.452	
1431+3146	A1930	1	51	+67	0.1312	16.27	17.58	I,S(F)	0.00	0.00	16.06	16.91	4.595	Bootis
1055+5702	A1132	1	149	+54	0.1345	16.15	17.55	I,S(E)	0.00	0.00	15.93	16.86	4.606	UMa#2
1153+2341	A1413	3	225	+77	0.1426	(15.70)	(17.13)	I,S(VP)	0.00	0.00	(15.46)	(16.40)	4.631	
1641+1327	A2224	3	358	+34	0.1499	17.01	18.59	S	0.15	0.20	16.61	17.62	4.652	
1534+3749	A2100	3	61	+54	0.1532	16.82	18.29	I(G)	0.00	0.00	16.55	17.51	4.662	
0025+2223	A31	2	115	-40	0.1594	16.94	18.44	I(E)	0.09	0.12	16.58	17.51	4.680	
1228+1050	A1553	2	285	+73	0.1651	17.19	18.68	I(E)	0.00	0.00	16.90	17.84	4.695	Virgo#3
0138+1832	A234	1	139	-43	0.1730	17.54	19.15	I(E)	0.06	0.09	17.17	18.17	4.714	
1309-0105	A1689	4	313	+61	0.1745	17.24	18.63	I,S(F)	0.00	0.00	16.93	17.73	4.719	
1304+3110	A1677	2	82	+85	0.1831	(17.24)	(18.79)	I(P)	0.00	0.00	(16.90)	(17.85)	4.740	
0925+2044	A801	2	209	+43	0.1917	16.96	18.64	I(G)	0.06	0.09	16.54	17.57	4.760	
1253+4422	A1643	1	121	+73	0.1979	18.04	19.64	S	0.00	0.00	17.66	18.63	4.774	
0855+0321	A732	1	226	+29	0.2018	17.68	19.28	I(G)	0.22	0.29	17.07	17.96	4.782	Hydra
1447+2617	...	(2)	37	+63	0.36	19.85	21.34	S(G)	0.00	0.00	18.77	19.79	5.033	
0024+1654	...	(2)	115	-45	0.38	19.55	(20.98)	S	0.04	0.06	18.34	(19.30)	5.057	
3C31	...	(0)	127	-30	0.0169	12.14	13.33	S	0.21	0.27	11.90	12.98	3.706	N383
3C40	A194	0	142	-63	0.0180	12.27	13.30	S(F)	0.00	0.00	12.24	13.21	3.732	N545
3C66	A347	0	140	-17	0.0215	12.90	13.86	S(P)	0.18*	0.24*	12.69	13.52	3.810	
3C465	A2634	1	104	-33	0.0301	(13.28)	(14.40)	I,S(G)	0.17	0.22	(13.06)	(14.03)		N7720
3C338	A2199	2	63	+44	0.0303	12.63	13.46	S(G)	0.05	0.07	12.53	13.23	3.958	N6166
3C317	A2052	0	9	+50	0.0351	13.44	14.51	S(F)	0.00	0.00	13.38	14.33	4.022	
M23-112	(A2638)	2	66	-64	0.0825	15.46	16.56	S(G)	0.00	0.00	15.33	16.14	4.394	
3C219	...	(2)	174	+45	0.1745	17.26	18.76	S(P)	0.07	0.09	16.88	17.77	4.719	
3C28	A115	3	124	-37	0.1959	17.59	19.01	S(F)	0.12	0.16	17.10	17.85	4.769	
3C295	1410+5226	(1)	97	+61	0.461	20.11	21.53	I,S(G)	0.00	0.00	18.63	19.63	5.141	

*Redshifts for Virgo and Fornax are mean values in different assumptions discussed in the text. Absorption values marked are estimated from the measured B - V colors.

The Abell (1958) cluster designation, or occasionally a more common name, is given in column (2) of table 2; column (3) is the richness class R, either listed by Abell or, if estimated here, it is in brackets; columns (4) and (5) list the galactic coordinates; (6) is the adopted mean cluster redshift; (7) and (8) show the final V_{26} and B_{26} standard metric magnitudes; and column (9) shows the method by which the aperture correction was made. The V_{26} and B_{26} magnitudes refer to the uncontaminated magnitude of the first-ranked cluster member. If the galaxy has a companion or a star that was included in the photometry, the measured values were corrected to that of the primary galaxy alone by using the Δ mag values listed in the final column of table 1.

b) Interstellar Absorption

An unconventional absorption correction has been used, based on the recent evidence that the average reddening in the galactic poles is statistically small, and on the premise that there is no nonselective absorption. Studies of the problem include those of McNamara and Langford (1969), Gottlieb and Upson (1969), Sandage (1964, 1969), Helfer and Sturch (1970), Peterson (1970*a*), Alexander and Carter (1971), and especially McClure and Crawford (1971). A summary discussion with references is given by Philip and Tifft (1971).

The evidence supports a model where the reddening in the polar cap ($|b| \gtrsim 50°$) is generally zero, and remains small for all $|b| \gtrsim 20°$. Such a model is provided by McClure and Crawford (1971, fig. 2) if their Z/Y ratio is suitably adjusted. We take $Z/Y \equiv \tan b_0$ to correspond to a reddening-free cap from $b = 50°$ to the pole. For a uniform-density slab (i.e., no Z dependence) centered on the plane it follows that

$$E(B - V) = \text{const.}\ [\tan b_0 - \tan b] \csc b\,, \tag{1}$$

for $|b| \leq 50°$, and zero otherwise.

The value of the constant depends on the half-thickness of the galactic layer. We choose to normalize for agreement with the Hubble half-thickness of ~ 0.25 mag in B, and adopt absorptions of

$$A_V = 0.165\,(1.192 - \tan b) \csc b\,, \tag{2}$$

$$A_B = 1.33 A_V\,, \tag{3}$$

for $|b| \leq 50°$.

This solution is only slightly incompatible with galaxy counts that conventionally give $A_B \simeq C(\csc b - 1)$, where C varies between 0.25 mag (Hubble 1934) and ~ 0.50 mag (Shane and Wirtanen 1954, 1967; also see de Vaucouleurs and Malik 1969; and especially Noonan 1971*a*). As Noonan points out, "if galactic absorption is (primarily) due to large (discrete interstellar clouds), then galaxy counts at low galactic latitudes, although conforming more or less to a cosecant law, need not be related to the polar galactic absorption."

The situation may be similar to that prevailing when broken cumulus clouds are scattered in an otherwise clear terrestrial sky. The clouds crowd toward the horizon, often leaving large patches of blue in the zenith. Although the optical path through them will follow a csc b law statistically, the zenith is mostly clear because it takes only *half* the area of the sphere for sec z to change from 1 to 2 ($90° \geq b \geq 30°$), and the zones of equal Δ sec z are stacked progressively closer to the horizon as sec z increases.

All regions of the galactic polar cap are not absorption-free as shown by the ridges of finite optical polarization found by Mathewson and Ford (1970) at high latitudes, but the available evidence does favor reddening-free cap on the average. Since there is no evidence for nonselective extinction, we adopt equations (2) and (3) as the correction to V_{26} and B_{26} for galactic absorption. The individual values are listed in columns (10) and (11) of table 2.

c) The K-Correction

Because of the radial color gradient in E and S0 galaxies, Whitford's (1971; see also Schild and Oke 1971) corrections for K-dimming are used rather than those of Oke and Sandage (1968). A slightly smoothed version of Whitford's table 3 has been adopted, and these values have been applied to the V_{26} and B_{26} data of table 2 to obtain the final corrected magnitudes listed in columns (12) and (13).

The resulting (m, z) number-pairs for some clusters differ[1] from the preliminary values given to Peach for his discussion of the ways to q_0 (Peach 1970) for two reasons. (1) In 1967 I had used the simpler approximation to the aperture correction of $\theta z =$ const., which takes no account of the difference between metric and isophotal diameters, or of the dependence of the correction on q_0 itself (Paper I, § V). (2) The K-corrections used in 1967 were those of Oke and Sandage (1968).

IV. PHOTOMETRY BY WESTERLUND AND WALL BY PETERSON

a) Data by Westerlund and Wall

Photometry by Westerlund and Wall (1969, hereafter called WW) has been published for radio sources, among which are 10 galaxies that are brightest members of aggregates. Corrections for aperture effect, absorption, and K-dimming have been applied to their data by the precepts of § III, and the results are listed in table 3. Richness classes for the 10 cases have been estimated by inspection of plate material, and are listed in column (2).

The first entry, 0036+03, is in the G194 group of HMS (table 11), as is 0153+05 (G741 group), 2318+07 (G7619), and 2247+11 (G7385). The most important aggregate is centered on NGC 4696 (1245−41), which is a rich cluster that is well shown on the Whiteoak extension of the Palomar charts. Redshifts of member galaxies were measured at Mount Stromlo in 1968, and the listed $\langle z \rangle$ is the mean of 13 values. The cluster 0131−36 has been described by Westerlund and Smith (1966). The source 1332−33 is IC 4296, which is at the center of a group of E galaxies, as is 1400−33 (NGC 5419), both of which appear on the *Palomar Sky Survey* prints.

Table 3 contains all WW groups and clusters not otherwise included in table 2. The magnitudes of 0153+05 and 0915−11 (Hydra A) have been corrected for contamination by companions. Hydra A is a dumbbell with Δ mag = 1.5 between the components.

b) Peterson's Data

Peterson (1970*a*) has published redshifts and magnitudes for many bright Abell clusters as observed with the 100- and 200-inch reflectors at Mount Wilson and Palomar. Of his 48 listed clusters, 11 are common to table 2, and an additional four are double or are contaminated by stars, leaving 33 new clusters considered here.

Correction for aperture effect by the present precepts could not be made, but Peterson does correct to a standard metric diameter using a $q_0 = \frac{1}{2}$ growth curve that he constructed from observations of NGC 383. (Over the range of redshifts covered by the data, the difference between a $q_0 = \frac{1}{2}$ and $q_0 = 1$ growth curve is insignificant.) His standard size is $\log \theta z = 0.14$, compared with $\log \theta z = 0.47$ adopted here (in the $z \to 0$ limit). This difference causes a zero-point shift in the magnitude system that is estimated to be $\Delta m = 0.30$ mag from figure 6 of Paper I. However, this value would be correct only if the shapes of Peterson's curve and of figure 6 in Paper I were identical. Without testing this, we have determined the difference empirically by comparing the separate Hubble diagrams (§ V) for each data sample. The correction found in this way is Δ mag = 0.39 mag, which has been applied to Peterson's V values to give $V(0.39)$ listed in table 4, together with the absorption correction of equation (2), and the K-dimming of § III.

[1] The differences are not gross, but they will vary systematically with z. Because Solheim and Tinsley (1972), McVittie (1972), and Vignato and Marcucci (1971) used values published by Peach (1970), which are earlier versions of those now listed in table 2 here, the conclusions of these authors will be affected to varying degrees. The data they used are not correct.

TABLE 3

WESTERLUND AND WALL RADIO GALAXIES IN CLUSTERS OR GROUPS WHICH ARE NOT DUMBBELLS OR IN TABLE 2

Source (1)	Richness (2)	l^{II} (3)	b^{II} (4)	z (5)	V_{26} (6)	B_{26} (7)	A_V (8)	A_B (9)	V_C (10)	B_C (11)	log cz (12)	Remarks (13)
0036+03.....	(0)	117	−59	0.0145	12.13	13.17	0.00	0.00	12.11	13.10	3.697	N193
0131−36.....	(0)	261	−77	0.0298	13.24	14.26	0.00	0.00	13.19	14.11	3.951	
0153+05*.....	(0)	153	−53	0.0188	11.95	12.99	0.00	0.00	11.98	12.96	3.751	N741
0915−11*.....	(0)	243	+25	0.0522	13.71	14.78	0.28	0.38	13.58	14.38	4.194	Hydra A
1245−41†.....	(2)	302	+22	0.0113†	11.05	12.07	0.15	0.20	10.90	11.87	3.498	N4696
1332−33.....	(0)	313	+28	0.0114	10.89	11.93	0.00	0.00	10.87	11.88	3.535	IC 4296
1400−33†.....	(0)	320	+27	0.0138‡	11.18	12.23	0.15	0.20	11.01	11.97	3.617	N5419
2152−69.....	(0)	322	−41	0.0266	13.31	14.30	0.09	0.11	13.19	14.06	3.902	
2247+11.....	(0)	82	−41	0.0268	12.53	13.61	0.09	0.11	12.40	13.37	3.906	N7385
2318+07§.....	(0)	88	−48	0.0118	10.99	12.03	0.01	0.01	10.96	11.96	3.550	N7626

* V_C and B_C corrected for Δmag = 3.1 mag companion for 0153 and 1.5 mag companion for 0915.

† NGC 4696, which is brightest member of Centaurus cluster. Redshift is mean of 13 member galaxies observed at Mount Stromlo during 1968–1969.

‡ Redshift of NGC 5419 obtained at Mount Stromlo with the 74-inch.

§ N7626 is second brightest member of N7619 group. Δmag = 0.3 which is applied.

TABLE 4

ADOPTED PHOTOMETRIC DATA FOR 33 FIRST RANKED GALAXIES IN CLUSTERS STUDIED BY PETERSON

CLUSTER (1)	OTHER (2)	Richness (3)	l^{II} (4)	b^{II} (5)	z (6)	$V_p(0.39)$ (7)	A_V (8)	K_V (9)	$V_c(.39)$ (10)	log CZ (11)
A76	IC1565	0	117	-56	0.0377	13.44	0.00	0.06	13.38	4.053
119*		1	126	-64	0.0387*	13.89	0.00	0.10	13.79	4.067
147		0	131	-60	0.0441	14.35	0.00	0.07	14.28	4.122
262		0	137	-25	0.0168	12.15	0.28	0.03	11.84	3.702
278		0	139	-29	0.0904	15.56	0.22	0.15	15.19	4.433
376		0	147	-21	0.0487	14.33	0.37	0.08	13.88	4.165
505		0	132	+22	0.0543	14.04	0.34	0.09	13.61	4.212
539		1	196	-18	0.0267	13.35	0.20	0.04	13.11	3.904
548		1	230	-24	0.0391	13.74	0.30	0.06	13.38	4.069
553		0	165	+14	0.0670	15.05	0.25	0.11	14.69	4.303
569	N2329	0	169	+23	0.0193	12.32	0.32	0.03	11.97	3.763
576		1	161	+26	0.0404	13.98	0.14	0.07	13.77	4.084
592		1	210	+16	0.0621	14.81	0.30	0.10	14.41	4.270
634		0	159	+34	0.0266	13.22	0.15	0.04	13.03	3.902
671	IC2378	0	193	+33	0.0497	13.84	0.17	0.08	13.59	4.173
754		2	239	+25	0.0537	13.95	0.28	0.09	13.58	4.207
993		0	249	+42	0.0530	14.09	0.07	0.09	13.93	4.201
1060	N3309	1	270	+27	0.0115	11.21	0.26	0.02	10.93	3.538
1139		0	251	+53	0.0376	13.81	0.00	0.06	13.75	4.052
1213		1	201	+69	0.0287	13.85	0.00	0.05	13.80	3.935
1228	IC2738	1	187	+69	0.0344	13.71	0.00	0.06	13.65	4.014
1257		0	183	+70	0.0339	14.13	0.00	0.05	14.08	4.007
1314	IC712	0	152	+64	0.0335	13.26	0.00	0.05	13.21	4.002
1318	N3737	1	144	+59	0.0189	12.36	0.00	0.03	12.33	3.753
1367	N3842	2	234	+73	0.0204	12.17	0.00	0.03	12.14	3.787
1736		0	313	+35	0.0431	13.94	0.14	0.07	13.73	4.112
2147		1	29	+45	0.0351	13.47	0.04	0.06	13.37	4.022
2152		1	30	+44	0.0440	14.01	0.05	0.07	13.89	4.121
2162	N6086	0	49	+46	0.0318	13.09	0.04	0.05	13.00	3.980
2197	N6173	1	65	+44	0.0322	12.81	0.05	0.05	12.71	3.985
2319		1	76	+14	0.0549	14.39	0.25	0.09	14.05	4.217
2657		1	97	-50	0.0414	14.38	0.00	0.07	14.31	4.094
2666	N7768	0	107	-34	0.0273	12.56	0.15	0.04	12.37	3.913

*Redshift quoted by Peterson in A119 is that of 3C29 which is evidently not a cluster member. Listed redshift is from a new spectrogram of the brightest cluster member taken at Mount Stromlo in 1969.

The only other point to be made before discussing the Hubble diagram for the various samples concerns possible abnormalities of the optical flux for those galaxies in tables 2, 3, and 4 that are themselves radio sources. Most radio galaxies have the optical appearance of normal elliptical or S0 systems. The contrary opinion is sometimes stated because sources such as Per A (NGC 1275), Vir A (M87), 3C 231 (M82), and Cen A (NGC 5128) have spectacularly abnormal forms. However, nearly all radio galaxies of Paper III have normal optical appearance, and most show the same distribution of $B_c - V_c$ colors as normal ellipticals.

Figure 1 shows the color distribution for galaxies in tables 2 and 3. The histograms for radio and nonradio galaxies are substantially the same, except for Per A at $B_c - V_c = +0.59$. The blueness here is due to abnormally strong emission lines of an intensity not found in the majority of radio sources. Because of figure 1, and because

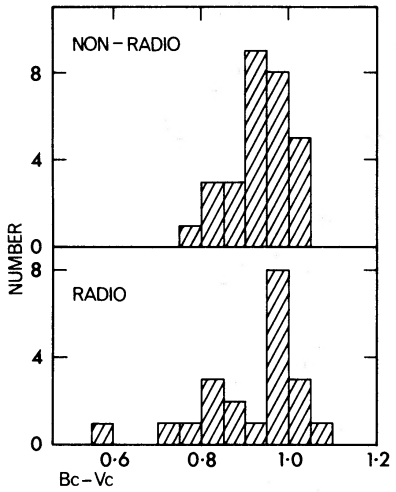

FIG. 1.—Distribution of the color index, after correcting for redshift, of radio and nonradio galaxies in tables 2 and 3. The outriding radio galaxy at $B_c - V_c = 0.59$ is NGC 1275, which has abnormally bright, wide spectral emission lines.

the (m, z) diagram for radio and nonradio galaxies is the same (cf. § V), there is no reason to delete those systems that qualify as first-ranked cluster members in discussions of the Hubble diagram. The events that give rise to the radio phenomenon do not, apparently, affect the optical flux generally.

V. THE HUBBLE DIAGRAM

It is shown later that the internal accuracy of the magnitudes is different for the three data samples. Because of this, the Hubble diagram will be discussed separately for each data group (tables 2, 3, and 4). Figure 2 shows the (m, z) relation for the 41 clusters measured in the present program (table 2). The data extend from the Virgo cluster[2] at $\log cz \simeq 3.056$ in the lower left corner to 3C 295 at $z = 0.461$. A line of slope 5 is drawn, as required in all homogeneous models in the $z \to 0$ limit, and the agreement with the observations is satisfactory. The equation of the line is

$$V_c = 5 \log cz - 6.76 , \qquad (4)$$

where the constant has been adjusted for zero mean residuals about the line.

The most remarkable feature of the diagram is the small scatter. Sources of the scatter are discussed later (§ VI), and it need only be remarked here that the two galaxies with the largest residuals are NGC 4889 in the Coma cluster, and the brightest galaxy in Cl 1153+2341. Each of these has an abnormal growth curve and Cl 1153 has a conspicuous extended halo to its optical image. They are the most obvious cases in our sample of the "supergiant cD" group discussed by Morgan and Lesh (1965). The fact that these two galaxies stand farthest to the left of the line in figure 1 argues that at least part of the scatter is due to variation in the absolute magnitude of the text galaxies, which, to be sure, is the usual assumption made on other grounds. Because such galaxies can be recognized easily by inspection of plates, we can, without

[2] It was previously mentioned that the mean redshifts of the Virgo and the Fornax clusters are uncertain. Two redshift values are plotted for each of these clusters in figure 1, corresponding to $z = 0.00379$ and $z = 0.00317$ for Virgo, and $z = 0.0048$ and $z = 0.0051$ for Fornax as discussed earlier. A new discussion by Tammann (1972) favors $cz = 1142$ km s^{-1} or $\langle z \rangle = 0.00381$ for Virgo.

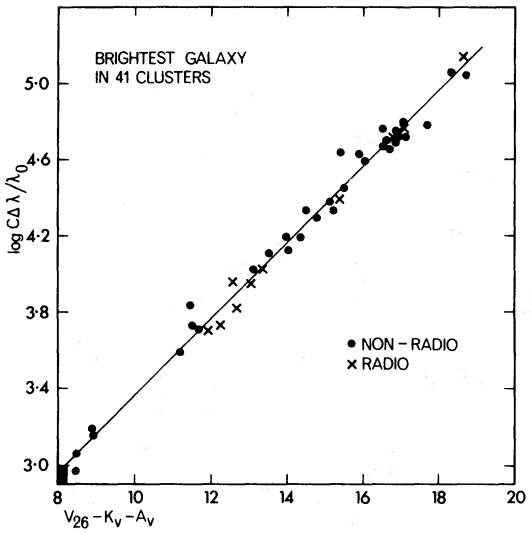

FIG. 2

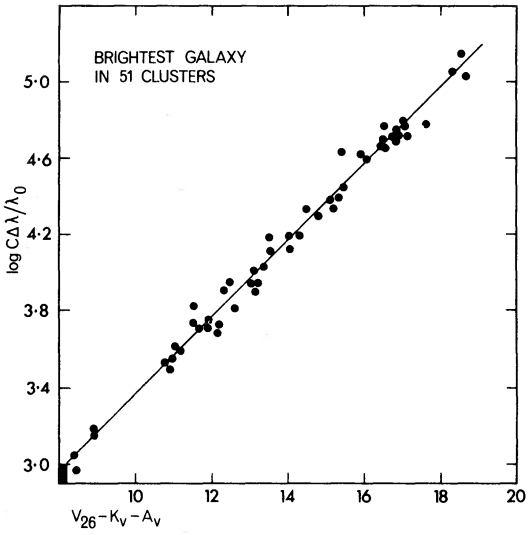

FIG. 3

FIG. 2.—The Hubble diagram for first-ranked galaxies in 41 clusters from the data of table 2. *Abscissa*, the corrected V_c magnitude; *ordinate*, the logarithmic redshift. The box in the lower left is the approximate interval within which Hubble established the redshift-distance relation in 1929. A line of slope 5, required by all homogeneous models in the $z \to 0$ limit, is fitted to the data in zero point only. It is equation (4) of the text.

FIG. 3.—Same as fig. 1, with data from table 3 added to those of table 2.

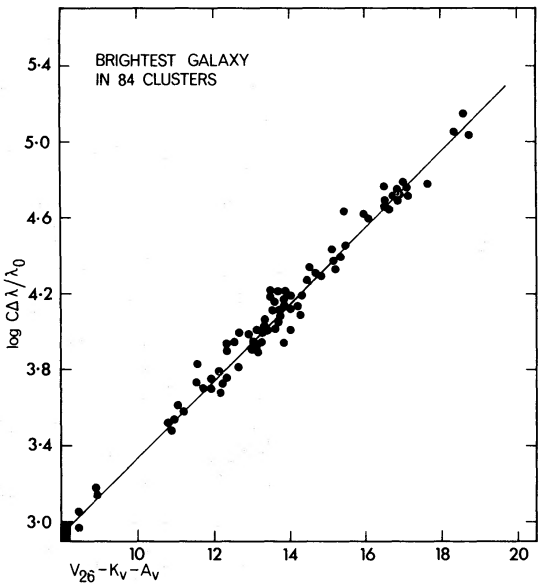

FIG. 4.—Same as fig. 1 for the combined data of tables 2, 3, and 4

bias, eliminate them *a priori* when the Hubble diagram is used for solutions of cosmological parameters.[3]

Figure 3 is the same as figure 2 except that the 10 groups and clusters of Westerlund and Wall have been added. The data fit well on the same Hubble line (eq. [4]), and partially fill the sparsely populated part of the diagram between the Fornax cluster ($cz = 1530$ km s^{-1}) and Coma ($cz \simeq 6660$ km s^{-1}).

Figure 4 is the same as figure 3 except that the 33 clusters of Peterson are added. The principal effect is to increase the scatter of the diagram near $\log cz \simeq 4.2$. Formal analysis of the scatter (presented later) confirms the difference in rms deviation between the samples, and shows that new observations could significantly improve the data of table 4, presumably if made at a darker site than Mount Wilson.

VI. ANALYSIS OF THE SCATTER

The scatter in figures 2–4 is due to a variety of causes. Among these are (1) errors in measurement of magnitudes (measuring errors of redshifts are generally negligible); (2) noncosmological redshift effects Δz caused by (*a*) virial velocities of galaxies within the clusters that are not averaged to zero if redshifts of only a few galaxies are measured, (*b*) virial and/or random velocities of the cluster centers themselves relative to the local expansion field, and (*c*) possible non-Doppler redshifts of unknown cause within the galaxies; (3) dispersion in absolute magnitude of galaxies in the sample; and (4) patchy intergalactic absorption, if any.

We cannot separate these effects by a study of the Hubble diagram alone, but we can put limits on the effects that combine to produce the total dispersions in redshift and in apparent magnitude, respectively, by reading the residuals in figures 2–4 vertically and horizontally.

a) Limit on Noncosmological Redshift Effects Δz

i) *Discussion*

If we put to zero all effects that cause scatter in the magnitudes, the residuals $\Delta \log z$ (read vertically) will be upper limits to any real redshift effect. The data are sufficiently numerous here to analyze the nature of the scatter in figures 2–4 for constraints on the possible causes of redshift residuals. We restrict the discussion to figures 2 and 3 where the data are of comparable accuracy.

Inspection of the diagrams shows that the vertical dispersion $\Delta(\log z)$ does not change with z; i.e., the envelope lines are parallel. The data are set out directly in figure 5, where it is clear that $\Delta \log z \neq f(z)$. This requires that $\Delta z/z = \text{const.}$, or $\langle \Delta z \rangle \propto z$, showing that any redshift effect Δz that is large enough to affect figures 2–4 cannot be internal to the individual galaxies because Δz would have to be proportional to distance to satisfy the observations. Such an effect has no rational explanation, and the conclusion is that most of the scatter in figures 2–4 must be due to effects on the magnitudes.

There must, of course, be *some* noncosmological redshift component Δz due to virial motions between clusters of galaxies and/or any initial random motions in the

[3] The three most prominent "cD" galaxies in our sample are Coma, Cl 1153+2341, and 3C 338 (Abell 2199). These galaxies are brighter than the mean of the sample by $\langle \Delta M_V \rangle = -0.76$ mag. However, there are seven such galaxies in table 2 as classified by Matthews, Morgan, and Schmidt (1964). The average for the group (3C 40, 3C 219, 3C 317, 3C 338, 3C 465, Cl 1153, and Coma) is $\langle \Delta M_V \rangle = -0.26$ mag, which is hardly significant. Galaxies such as 3C 40 ($\Delta M_V = +0.34$ mag), 3C 219 (+0.04), 3C 317 (+0.03), and 3C 465 (0.04) have slightly fainter absolute magnitudes than the mean. Except, then, for a few galaxies with abnormally large and easily recognized envelopes, there is little peculiar about the "cD" systems in our sample.

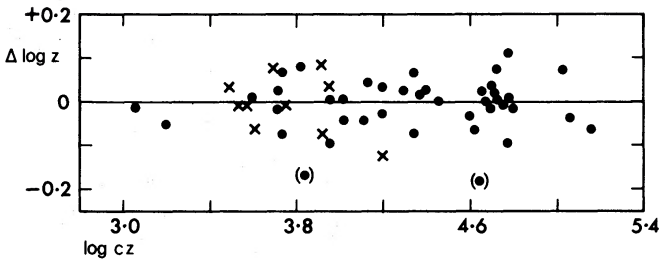

FIG. 5.—Distribution of residuals from fig. 2, read vertically (as $\Delta \log z$ at constant V_c) as a function of z. Data are from tables 2 and 3; the values can be taken explicitly from table 5 using the relation $\Delta \log z = -0.2\,\Delta M_V$. *Crosses*, from table 3; *dots*, from table 2.

early Universe that has not been damped to small values by the expansion. We can set an upper limit to Δz by considering the distribution of $\Delta \log z$ in the present data.

The histogram of $\Delta \log z$ from all data in tables 2, 3, and 4, shown in figure 6, is a symmetrical Gaussian with $\sigma(\Delta \log z) = 0.063$. An even narrower distribution with $\sigma(\Delta \log z) = 0.50$ describes the data of table 2 alone. The upper limit to any redshift dispersion is then

$$\sigma(\Delta z/z) = 0.115\,. \tag{5}$$

Because this limit holds for all z, it holds for any z. In particular, if there is no local shear at the Virgo cluster (fig. 2), it holds at $cz = 1000$ km s^{-1}, from which it follows from equation (5) that $\sigma(\Delta\, cz) \lesssim 115$ km s^{-1} as the upper limit on the distribution of random velocities.

ii) *Conclusions*

1. If all scatter in the Hubble diagram were due to a redshift residual Δz, then it would have to vary linearly with distance. Because this is unreasonable, it follows that most of the scatter for first-ranked cluster galaxies is caused by scatter in the magnitudes.

2. An upper limit of $\sigma(\Delta\, cz) \simeq 100$ km s^{-1} can be put on the distribution of random velocities of cluster centers (assuming that the listed cz values in tables 2–4 do, in fact, refer to the centers). Redshifts vary monotonically with distance to within this limit. There is no evidence from the cluster data that Δz is other than zero.

b) Dispersion in the Magnitudes

i) *Discussion*

The residuals ΔV_c calculated from equation (4) are listed for each cluster in table 5. Also listed for later use is the richness class R (Abell 1958), and $\log cz$. These residuals are caused by all effects that can randomly affect the apparent luminosities.

The statistics of the residuals of table 5 show that the data samples are of unequal weight. The data of table 2 (when the two abnormal cD clusters of Coma and Cl 1153+2341 are omitted for the previously mentioned reason) are well fitted by a symmetrical Gaussian with $\sigma(\Delta V_c) = 0.252$ mag for 39 clusters. The good fit to equation (4) is shown by $(\Delta V_c) = -0.003 \pm 0.040$ mag for these data. Adding the 10 groups and clusters of table 3 gives $\langle \Delta V_c \rangle = -0.009 \pm 0.038$ mag with $\sigma = 0.269$ mag for 49 cases. Data from table 4 alone give $\langle \Delta V_c \rangle = 0.000 \pm 0.066$ mag with $\sigma(\Delta V_c) = 0.377$ (33 cases).

Table 5

Magnitude Residuals for 84 Brightest Cluster Galaxies

NAME	R	Log cz	ΔV_c*	NAME	R	Log cz	ΔV_c	NAME	R	Log cz	ΔV_c
(1)	(2)	(3)	(4)	(1)	(2)	(3)	(4)	(1)	(2)	(3)	(4)
FROM TABLE 2											
VIRGO	(1)	3.056	-0.07	0024 +16	(2)	5.057	-0.18	A278	0	4.433	-0.22
FORNAX	(1)	3.184	-0.26	3C 31	(0)	3.706	+0.13	A376	0	4.165	-0.18
PEG I	(0)	3.584	+0.04	3C 40	0	3.732	+0.34	A505	0	4.212	-0.69
0122 +33	(1)	3.710	-0.09	3C 66	0	3.810	+0.40	A539	1	3.904	+0.35
PERSEUS	2	3.735	-0.38	3C 465	1	3.956	+0.04	A548	1	4.069	-0.20
COMA	2	3.824	-0.85	3C 338	2	3.958	-0.50	A553	0	4.303	-0.06
HER	2	4.017	-0.20	3C 317	0	4.022	+0.03	A569	0	3.763	-0.08
2308 +07	(0)	4.109	-0.22	M23 -112	2	4.394	+0.12	A576	1	4.084	+0.11
2322 +14	0	4.120	+0.24	3C 219	(2)	4.719	+0.04	A592	1	4.270	-0.18
1145 +55	1	4.191	+0.20	3C 28	3	4.769	+0.02	A634	0	3.902	+0.28
0106 -15	1	4.198	-0.20	3C 295	(1)	5.141	-0.32	A671	0	4.173	-0.52
1024 +10	1	4.290	+0.12					A754	2	4.207	-0.70
1239 +18	0	4.333	-0.38	FROM TABLE 3				A993	0	4.201	-0.32
1520 +27	2	4.334	+0.33					A1060	1	3.538	0.00
0705 +35	0	4.369	+0.06	0036 +03	(0)	3.697	+0.38	A1139	0	4.052	+0.25
1513 +04	1	4.452	0.00	0131 -36	(0)	3.951	+0.20	A1213	1	3.935	+0.88
1431 +31	1	4.595	-0.16	0153 +05	(0)	3.751	-0.01	A1228	1	4.014	+0.34
1055 +57	1	4.606	-0.34	0915 -11	(0)	4.194	-0.63	A1257	0	4.007	+0.80
1153 +23	3	4.631	-0.94	1245 -41	(2)	3.498	+0.17	A1314	0	4.002	-0.04
1641 +13	3	4.652	+0.11	1332 -33	(0)	3.535	-0.04	A1318	1	3.753	+0.32
1534 +37	3	4.662	0.00	1400 -33	(0)	3.617	-0.32	A1367	2	3.787	-0.04
0025 +22	2	4.680	-0.06	2152 -69	(0)	3.902	+0.44	A1736	0	4.112	-0.07
1228 +10	2	4.695	+0.18	2247 +11	(0)	3.906	-0.37	A2147	1	4.022	+0.02
0138 +18	1	4.714	+0.36	2318 +07	(0)	3.550	-0.03	A2152	1	4.121	+0.04
1309 -01	4	4.719	+0.10					A2162	0	3.980	-0.14
1304 +31	2	4.740	-0.04	FROM TABLE 4				A2197	1	3.985	-0.46
0925 +20	2	4.760	-0.50					A2319	1	4.217	-0.28
1253 +44	1	4.774	+0.55	A76	0	4.053	-0.12	A2657	1	4.094	+0.60
0855 +03	1	4.782	-0.08	A119	1	4.067	+0.22	A2666	0	3.913	-0.44
1447 +26	(2)	5.033	+0.36	A147	0	4.122	+0.43				
				A262	0	3.702	+0.09				

* The sense of ΔV_c is observed minus calculated, using equation (4). Redshift residuals discussed in § VI are found from $\Delta \log z = 0.2\ \Delta V_c$.

The difference in dispersion between the samples must be due mainly to differing observational errors. It seems likely that this is caused by the more unfavorable night-sky level on Mount Wilson (table 4) than on Palomar (table 2) or Siding Spring Mountain (table 3). If true, the interval errors of part of the material can be decreased with fair ease by new observations, but even so, the present data themselves force two principal conclusions.

ii) *Conclusions*

1. First-ranked cluster galaxies have a remarkably small dispersion in absolute magnitude.

2. Any intergalactic absorption in the path length of each of the clusters studied here cannot be patchy to within an upper limit described by $\sigma(A_v) \simeq 0.25$ mag, as obtained from figure 2 by putting all other causes of scatter to zero.

Furthermore, concerning point 2, there is no evidence for *selective* intergalactic absorption to within a limit of $\sigma[E(B-V)] \lesssim 0.05$ mag as set from the agreement of theory and observation on the color change with redshift of giant ellipticals (Oke and Sandage 1968, fig. 2). The evidence from the present data is, then, negative as regards the existence of general intergalactic absorption.

The distribution of magnitude residuals from all causes that spread the abscissa values is shown in figure 6 for the complete sample (table 5, omitting Coma and Cl 1153+2341) of 82 clusters. The dispersion of the best-fitting Gaussian is $\sigma(\Delta M_V) = 0.32$ mag, and the abscissa value for absolute magnitude has been calculated from

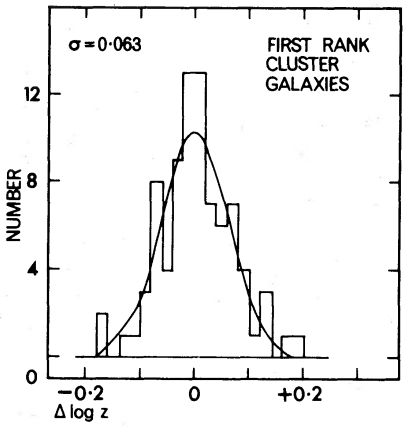

FIG. 6

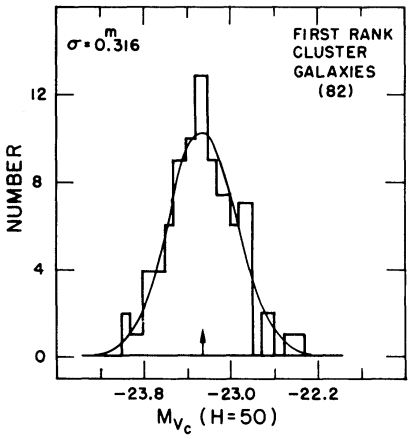

FIG. 7

FIG. 6.—Histogram of the Δ log z residuals for galaxies from tables 2 and 3, fitted with an equal-area Gaussian of $\sigma(\Delta \log z) = 0.063$.

FIG. 7.—Distribution of residuals from fig. 3 read horizontally (i.e., at constant log z) as ΔM_V. Data for 82 clusters of table 5 are compared with an equal-area Gaussian of $\sigma(\Delta M_V) = 0.316$ mag. Abscissa is absolute magnitude assuming equation (4) of the text and a Hubble constant of $H_0 = 50$ km s^{-1} Mpc^{-1}.

equation (4) using a Hubble constant of $H_0 = 50$ km s^{-1} Mpc^{-1}. The distribution would have been even narrower with $\sigma = 0.25$ mag if the data of table 2 alone had been used.[4]

VII. ABSOLUTE MAGNITUDE OF FIRST-RANKED CLUSTER GALAXIES AS A FUNCTION OF CLUSTER POPULATION: THE SCOTT EFFECT

The tightness of the luminosity function of bright cluster galaxies has been discussed or implied elsewhere (Hubble 1953; HMS 1956; Sandage 1968*a*, *c*), and much has been written on a possible dependence of M_V of the brightest cluster galaxy on the population of the parent cluster (Scott 1957; Peebles 1968, 1969; Peach 1969; Peterson 1970*b*, *c*). It is known that no gross difference in $\langle M_V \rangle$ exists between rich and poor clusters that differ in population by at least a factor of 100; otherwise the brightest members of the smallest HMS groups would not lie close to the mean line of figure 2. Examples from table 11 of HMS include NGC 128 (group with $N \simeq 5$ members), NGC 1600 (8), NGC 5077 (8), and NGC 5371 (5) where the (m_{pg}, z) data given there are consistent with the (B_c, z) equivalent of figure 1 to within $\langle \Delta M_V \rangle = \pm 0.5$ mag.

[4] There is one effect that tends to artificially *decrease* the scatter from its true value to that shown in figures 2–6, caused by the particular procedure that was used for the aperture correction. By Paper I, the first approximation to the correction requires that all program galaxies be identical in intrinsic linear diameter. Galaxies that are smaller than average will, in general, be fainter than average, and such galaxies will be corrected to be too bright by the correction procedure without iteration. Larger galaxies will be made too faint.

The size of this pseudo-decrease of the scatter is found by reading figure 6 of Paper I at the 1 σ points of $\Delta \log \theta = \pm 0.05$ away from the standard diameter marked in that diagram. The Δ mag at these points are only 0.05 mag, which is nearly negligible compared with the observed dispersion (figs. 2 and 7). The effect, although present in principle, is therefore not very important.

The analysis of the present data to test for any dependence of M_V within the gross division into the Abell (1958) richness classes is set out in table 6 for five combinations of the data. Listed as $\langle \Delta M_V \rangle$ is the mean difference of residuals calculated from equation (4), the rms error $\sigma/\sqrt{N}$ of this mean, the $\sigma(\Delta M_V)$ of the distribution, and the number of galaxies in the subsample. Table 6 reveals that there is no variation of $\langle \Delta M_V \rangle$ with R for the total sample, and further, that the individual values of $\langle \Delta M_V \rangle$ for all data groups are within $\sim 1\sigma$ of $\langle \Delta M_V \rangle = 0$. These results are shown in figure 8, which is the representation of tables 5 and 6.

The conclusion that $\langle \Delta M_V \rangle$ is independent of R agrees with that of Peach (1969), who used the data sample that was preliminary to part of table 2. It does not agree with the conclusion of Peebles (1969) or of Peterson (1970*b*), although the systematic variation claimed by these authors is not significant at the 1σ level. These authors primarily used the early table 2 results as published by Peach (1969), although Peterson (1970*c*) included his own values in his second discussion.

The reason for the contrary opinions can be seen by noting from table 6 that the systematic effect in $\langle \Delta M_V \rangle$ from data in table 2 is opposite to the trend from Peterson's data alone, and by adding the two groups the effect tends to cancel. However, it is clear that any effect, even if real, is minute, and is lost in the noise at the ± 0.05 mag level.

To this evidence we can add preliminary results to be discussed in Paper VII where the discrete variable R is replaced by the continuous population number N in groups and clusters, where $5 \leq N < 500$. The brightest galaxy in aggregates over this population interval has a ΔM_V that is consistent with the distribution of figure 7. The result is similar to but is more general than that mentioned earlier for certain of the HMS

TABLE 6

RESIDUALS FROM THE MEAN ABSOLUTE MAGNITUDE AS A FUNCTION OF RICHNESS CLASS FOR THE THREE DATA GROUPS*

GROUP	DATUM	R 0	1	2	3	4
Table 2, S.....	$\langle \Delta M_V \rangle$ (mag)	+0.071	−0.018	−0.069	+0.043	+0.10
	$\sigma/\sqrt{N}$	±0.084	±0.069	±0.085	±0.034	± ∼0.3
	$\sigma(\Delta M_V)$	0.251	0.256	0.294	...	...
	N	9	14	12	3	1
Table 3, W + W.....	$\langle \Delta M_V \rangle$	−0.042	...	+0.17	...	...
	$\sigma/\sqrt{N}$	±0.118	0	...	0	0
	$\sigma(\Delta M_V)$	0.354	...	...	...	...
	N	9	0	1	0	0
Tables 2 + 3, S + WW	$\langle \Delta M_V \rangle$	+0.014	−0.018	−0.051	+0.043	+0.10
	$\sigma/\sqrt{N}$	±0.071	±0.069	±0.080	±0.034	± ∼0.3
	$\sigma(\Delta M_V)$	0.303	0.256	0.289	...	...
	N	18	14	13	3	1
Table 4, P.....	$\langle \Delta M_V \rangle$	−0.061	+0.126	−0.37	...	...
	$\sigma/\sqrt{N}$	±0.088	±0.096	±0.33	...	...
	$\sigma(\Delta M_V)$	0.361	0.359	∼0.47	...	...
	N	17	14	2	0	0
Total: S + WW + P..	$\langle \Delta M_V \rangle$	−0.022	+0.054	−0.088	+0.043	+0.10
	$\sigma/\sqrt{N}$	±0.056	±0.060	±0.082	±0.034	± ∼0.3
	$\sigma(\Delta M_V)$	0.330	0.315	0.318	...	...
	N	35	25	15	3	1

* The sign convention is the same as for table 5. Negative sign means *brighter* than the mean line drawn in figures 2, 3, and 4.

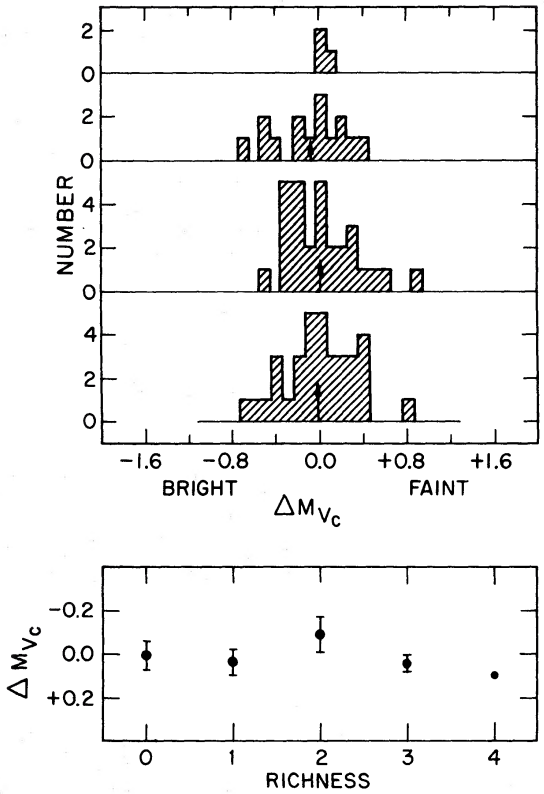

FIG. 8.—Correlation of $\langle \Delta M_V \rangle$ for each richness class of table 6 with the Abell richness class R. *Upper*, the histogram of the distributions for $R = 0$ to 3; *lower*, mean values as a function of R. Negative sign means magnitude is brighter than average.

groups. Apparently, then, there is a deeper significance to the luminosity of the first-ranked cluster E galaxy than that attributed by Peebles (1968, 1969) from his statistical theory of random variation of a universal luminosity function and a constant total mass to all clusters (which obviously is not the case).

These data lead to a principal conclusion of this paper: The luminosity of the brightest cluster member does not depend strongly, if at all, on the luminosities of the fainter cluster members. The luminosity function has a nearly vertical asymptote (to within $\sigma = 0.25$ mag), and is virtually independent of R.

This result, remarkable in itself, appears to be even more so because additional data that are presently available suggest a wider proposition. The ΔM_{1-j} between the first and the jth brightest cluster galaxy appears to be a function of cluster richness even though M_V (first) is not. The implications of these results, if true, is that a normal E galaxy apparently cannot be more massive than a critical upper limit, determined by some unknown physical cutoff. In rich clusters, several galaxies can have nearly this limiting mass; in poor aggregates, one such large galaxy almost always exists, but the second-ranked and fainter galaxies are far down on the luminosity function that applies to rich clusters. These results are not understood, but they would appear to be important clues to the process of galaxy formation.

To the extent that the results are generally valid (is the present sample typical?), there will be no bias in the Hubble diagram that would favor brighter-than-average galaxies at large redshift, caused by the observers choosing clusters of high richness R

[the Scott (1957) effect]. The absolute luminosity of the brightest galaxy does not depend on R.[5]

VIII. q_0 IN FRIEDMANN MODELS

If we assume that matter is distributed in a strictly homogeneous manner on every scale, and that the curvature is precisely constant everywhere, we can use idealized Robertson-Walker–like models together with the observations to obtain *formal* parameter values for quantities such as the cosmological constant Λ and q_0.[6] Analysis of such a solution is useful to show where new observations are needed, even if the idealized models are eventually found to require corrections.

In this section we restrict ourselves to Friedmann models ($\Lambda = 0$) because, within the range of z of our present data, the differences in the Hubble diagram between these and Lemaître models is very small (cf. Refsdal, Stabell, and de Lange 1967, figs. 1 and 2). A high degree of indeterminancy results if it is required to solve for both q_0 and Λ. We rest with Peach's (1970) discussion of the $\Lambda \neq 0$ case.

The analysis is elementary if $\Lambda = 0$. An exact two-dimensional least-squares solution can be made directly, rather than the linearized iterative procedure developed by Peach where three variables were optimized.

For $q_0 > 0$ Mattig's (1958) equation of the problem is

$$m = 5 \log q_0^{-2}\{q_0 z + (q_0 - 1)[(2q_0 z + 1)^{1/2} - 1]\} + C , \tag{6}$$

which holds for all redshifts and which accounts for the effects of light-travel time and deceleration.

For the $q_0 = 0$ case, the equation is

$$m = 5 \log z(1 + z/2) + C ; \tag{7}$$

and for $q_0 = -1$,

$$m = 5 \log z(1 + z) + C . \tag{8}$$

These equations were used in a direct search by computer for the minimum of the squared residuals

$$\sum_{i=0}^{n} (m_{\text{obs},i} - m_{\text{cal},i})^2 ,$$

using the data tables 2–4 as q_0 and C were varied progressively in steps of $\Delta q_0 = 0.1$ and $\Delta C = 0.02$ mag from appropriate starting values. The dispersion,

$$\sigma \equiv \left[\sum_{i=0}^{n} (\Delta m_i)^2/n\right]^{1/2} ,$$

for each q_0, C pair was displayed in a q_0, C matrix, and the minimum σ with its resulting q_0, C values was found by inspection of the array.

Solutions were made separately for the data of figures 2, 3, and 4. The optimum value of C was 20.62 mag for all cases. Figure 9 illustrates the run of $\sigma(q_0)$ for this C

[5] Two other distance criteria have been used occasionally. They are (1) the mean luminosity of the first, third, fifth, and tenth cluster galaxy as used by HMS, and (2) a hump in the cluster luminosity function suggested by Abell and Eastmond (1968). The HMS criteria will suffer from the Scott effect if $\langle \Delta M_{1-j} \rangle$ does indeed vary with R. For the Abell-Eastmond criteria to be more useful than the first-ranked cluster galaxy requires proof (*a*) that the hump is universal, (*b*) that $\sigma(M_{\text{hump}})$ is smaller than $\sigma(M_{1\text{st}})$ of figure 7, and (*c*) that $\langle M_{\text{hump}} \rangle$ is independent of richness, as in figure 8. That at least some of these requirements are not met is shown elsewhere (Sandage 1972*b*).

[6] The relation between this solution and reality requires, as previously mentioned, a Kristian-Sachs-like test.

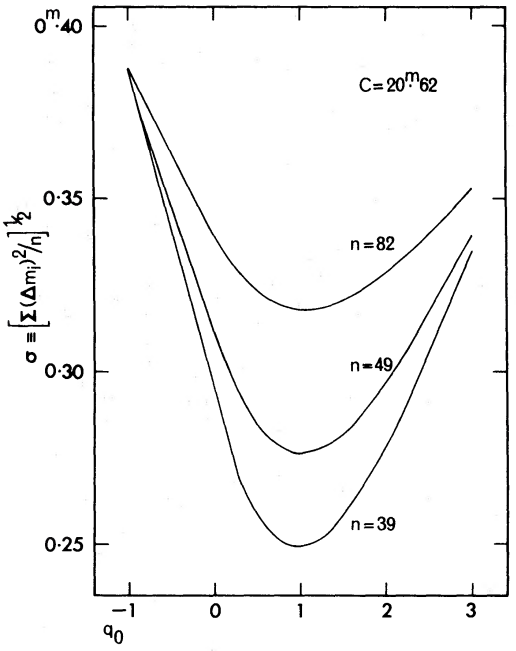

FIG. 9

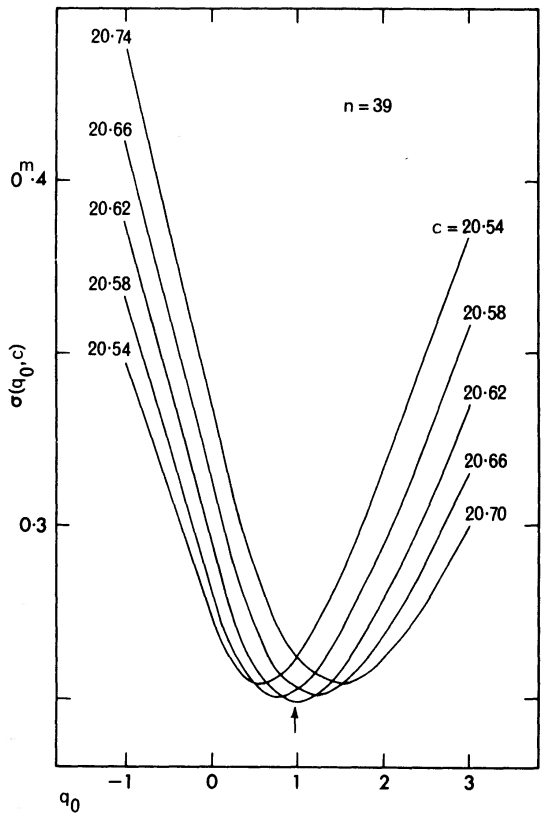

FIG. 10

FIG. 9.—Search for the minimum σ value by varying q_0 in equation (6), with $C = 20.62$ mag for three combinations of the cluster data.

FIG. 10.—Same as fig. 9 as both C and q_0 are varied about the optimized value, using data in table 2, with Coma and Cl 1153 omitted. Formal solution is $q_0 = 0.96 \pm 0.4$ (p.e.).

for the three data groups, as q_0 is varied from -1 to $+3$. The σ values at minimum in figure 9 are similar to those of table 6 (0.25 mag for the $n = 39$ case, $\sigma = 0.27$ mag for $n = 49$, and $\sigma = 0.316$ mag for $n = 82$).

Note that the most probable solutions are near $q_0 = +1$, and that the minimum is sharper for the highest-weight data ($n = 39$). This sharpness illustrates the importance (1) of using data of the highest observational accuracy, or, more to the point, (2) of using as test galaxies those with the smallest possible dispersion in intrinsic absolute luminosity.[7]

Figure 9 shows parts of the q_0, C matrix that contain the absolute minimum of the $\sigma(q_0, C)$ function. Near this minimum, the σ function varies slowly, and a range of q_0 is possible at various confidence levels. The depth of the $\sigma(q_0, C)_{\min}$ valley determines the probable error of the solution. The effect of varying C is shown in figure 10 for the $n = 39$ case, where the trial values are moved by σ (i.e., 0.04 mag) and 2 σ on either side of the optimum value. The probable error of q_0 is related to the steepness of the envelope to these curves.

[7] Radio galaxies are therefore not ideal test objects, as shown by figure 3 of Paper III that follows.

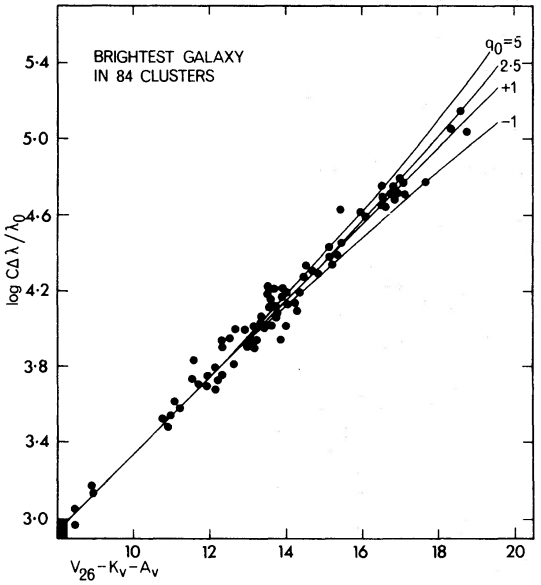

FIG. 11.—Same as fig. 3 with lines of constant q_0 superposed from equation (6), with C = 20.62 mag.

An approximate error analysis was made by calculating the value of χ^2 for each $\sigma(q_0, C)$. The parent distribution of residuals, taken as that at the minimum of figure 9 for $n = 39$ (essentially the Gaussian of fig. 7, but for the $n = 39$ case) was compared with the distribution at each other q_0, C value. The computer was programmed to sort each calculated set of residuals into 27 bins of 0.1 mag size for each row and column of the q_0, C matrix. There are 25 degrees of freedom with 27 bins, and the probabilities that the given χ^2 values could each come from the parent population can be put by the standard χ^2 test. This permits contours of given confidence levels to be drawn in the q_0, C array, and hence determines a probable error.

The method is noisy with only 39 (or even 82) clusters, because the run of χ^2 is not smooth throughout the matrix due to small-number statistics in the individual distributions. However, a general feel for the accuracy did come easily, and the rms error of the optimized q_0 value is estimated as $\simeq \pm 0.6$. This is essentially the same value obtained by Peach by a different method.

The final solution, using only the V_c data for 39 clusters in table 2, is then

$$q_0 = +0.96 \pm 0.4 \text{ (p.e.)}, \tag{9}$$

or, at the 2 σ level (95 percent confidence)

$$q_0 = 1 + 1. \tag{10}$$

The result that $q_0 \simeq +1$ can be appreciated from figure 11, where the solution is illustrated, showing the large divergence of the points from the curves for the $q_0 = -1$ and $q_0 = +3$ cases.[8]

[8] Our result differs from $q_0 = 0.3$ suggested by Baum (1972) from his study of diameter of galaxies in four clusters. Putting aside the question of the smallness of his sample in the presence of an intrinsic dispersion of $\Delta \log \theta \simeq 0.05$, which Baum does not discuss, a more serious conceptual problem exists. Baum clearly measures isophotal diameters, despite the fact that the driving cam of his device is calibrated in linear measure. The point is that the difference between isophotal and metric diameters is caused by the effect of redshift on surface brightness. It is intrinsic to the image of the galaxy; it occurs there and then under redshift, and cannot be removed by manipulation at the telescope here and now.

IX. CONSEQUENCES

1. If q_0 actually equals $+1$, the mean density ($\rho = 3\,H_0^2/4\pi\,G$) required to produce this deceleration is much higher than direct estimates of the luminous matter density. The problem has existed since the first estimates by Hubble (1926), and has not changed in the many rediscussions (cf. Shapiro 1971 with earlier references therein; see also Noonan 1971*b*). The discrepancy is a factor of ~ 50, requiring that $q_0 \simeq 0.02$ if there is no matter between the galaxies. No such matter in particular ionization states has been detected to quite significant limits (cf. Gunn and Peterson 1965; Bahcall and Salpeter 1965). Indeed, if such matter exists and is not transparent, the resulting extinction makes the measured m values fainter than the true, which requires q_0 (true) $> q_0$ (observed) for all cases. A particular model with electron scattering is discussed by Bahcall and May (1968).

2. The time to the Friedmann singularity is $0.57\,H_0^{-1}$ for $q_0 = +1$, which, with $H_0 = 55 \pm 7$ km s^{-1} Mpc^{-1} gives $T_F = (10 \pm 1.5) \times 10^9$ years. This is the same, to within the errors, as the age of the oldest galactic stars at $(10 \pm 3) \times 10^9$ years (Sandage 1970*a*). If $q_0 = 0$, then $T_F = 17.7 \times 10^9$ years. Intermediate values are $T_F = 11.8 \times 10^9$ years, for $q_0 = 0.5$, and $T_F = 13.6 \times 10^9$ years for $q_0 = 0.2$ (cf. table 8 of Sandage 1961*a*).

3. The correction not yet considered is the evolutionary change of luminosity in the look-back time. Agreement on its numerical value and on its sign has not yet been reached. Various theoretical estimates (cf. Tinsley 1968; Tinsley and Spinrad 1971) are higher than either (*a*) calculations from semiempirical evolutionary models that work backwards up the *H-R* diagram in the look-back time (Sandage 1961*b*, 1970*b*) or (*b*) calculations from direct observations of the reddening of the energy distribution of galaxies as a function of z (Oke and Sandage 1968; Oke 1971). Because the problem is not solved, we are content here to estimate how large dM/dt must be to change the present solution from $q_0 = +1$ to $q_0 = 0$.

Expansion of equation (6) in powers of z gives

$$m = 5 \log z + 1.086(1 - q_0)z + O(z^2) + C\,. \tag{11}$$

To make a change of $\Delta q_0 = 1$ requires that the magnitudes must be made fainter by $1.086z$. The proper look-back time for $q_0 = 0$ is, quite generally, $\tau = z(1 + z)^{-1}H_0^{-1}$, which requires that

$$dM/dt = 1.086(1 + z)H_0 \text{ mag year}^{-1}\,. \tag{12}$$

This equation shows that for $z = 0.461$ at 3C 295, with $H_0 = 55$ km s^{-1} Mpc^{-1}, then $dM/dt = 0.09$ mag per 10^9 years, in the sense that galaxies must be brighter in the cosmic past.[9]

This rate is large according to many models. The steepness of the luminosity function near $M_V = +4$ in models made explicit by Spinrad and Taylor (1971), for example, makes it unlikely that M fades by this amount during the look-back time, or even that the sign of dM/dt is correct. But uncertainties are still large enough that the question whether the evolutionary correction can change q_0 toward zero, if not to it, may still be open (but see Tinsley 1972).

4. No decision is yet possible at a high confidence level (~ 50 percent) as to whether the Universe is open or closed ($q_0 \lesssim \frac{1}{2}$), whether the expansion will stop or will continue forever ($q_0 \lesssim \frac{1}{2}$), or whether there is much missing mass ($q_0 > 0$). The only firm conclusions are: (1) the present data do not support an idealized steady-state model

[9] The $1 + z$ term in equation (12) shows merely that the rate of brightening (expressed in mag year^{-1}) is not linear with time. It is required to be larger in the past (i.e., at larger redshift) than now if the proposed change in the solution is to be exact.

that requires $q_0 = -1$, and (2) more data for clusters at large redshift are needed to make a more stringent solution.

X. SUMMARY

1. The Hubble diagram for first-ranked cluster galaxies has a small dispersion. Considered as a scatter in absolute magnitudes, an upper limit to the distribution is $\sigma(M_V) \simeq 0.25$ mag.

2. There is no evidence for intergalactic absorption, either patchy at the $\sigma = 0.25$ mag level, or general and selective at the $\sigma[E(B - V)] \simeq 0.05$ mag level.

3. The absolute luminosity of first-ranked cluster galaxies does not depend strongly, if at all, on the luminosity function of the fainter cluster members. This luminosity is independent of cluster richness for galaxies in the present sample, suggesting that there is an upper cutoff in galaxian mass that has a sharpness of $\sigma \simeq \pm 25$ percent.

4. Least-squares solutions for q_0 using idealized uniform models and the data for 39 clusters gives $q_0 = 0.96 \pm 0.4$ (p.e.). This can be reduced to $q_0 \simeq 0$ by a luminosity evolution given by equation (12). The solution cannot be considered secure until a test is made of how closely the idealized Friedmann models describe the actual Universe.

It is a pleasure to thank Milton Humason for his interest and encouragement in this work until 1963 when he retired from the Observatories. Special thanks go to Eugene Hancock and Al Olmstead at Mount Wilson, and Gary Tuton at Palomar for their efficient operation of the telescopes. Thanks to Ed Dennison and his personnel of the Astroelectronic Laboratory, the pulse-counting equipment and read-out systems at both Mount Wilson and Palomar were available, working, and important for the faint photometry. Malcolm Riley programmed the equations for the solutions for q_0 and the χ^2 test, and it is a pleasure to acknowledge his help.

It is a special pleasure to thank Professor O. J. Eggen for the hospitality of the Mount Stromlo and Siding Spring Observatories, Australia, where a draft of the paper was written, to thank the Australian-American Educational Foundation for a fellowship that made the Australian trip possible, and to acknowledge Jerome Kristian for discussions of the presentation of a first draft of this material.

REFERENCES

Abell, G. O. 1958, *Ap. J. Suppl.*, **3**, 211.
Abell, G. O., and Eastmond, S. 1968, *A.J.*, **73**, S161.
Alexander, J. B., and Carter, B. S. 1971, *R.O.B.*, No. 169, p. 353.
Bahcall, J. N., and May, R. M. 1968, *Ap. J.*, **152**, 37.
Bahcall, J. N., and Salpeter, E. E. 1965, *Ap. J.*, **142**, 1677.
Baum, W. A. 1962, *Problems of Extragalactic Research*, ed. G. C. McVittie (New York: Macmillan Co.), p. 390.
———. 1972, *I.A.U. Symposium No. 44*, Uppsala.
Bowen, I. S. 1957, *Carnegie Yrb.*, **56**, p. 62.
Gottlieb, D. M., and Upson, W. L. 1969, *Ap. J.*, **157**, 611.
Gunn, J., and Peterson, B. 1965, *Ap. J.*, **142**, 1633.
Helfer, H. L., and Sturch, C. 1970, *A.J.*, **75**, 971.
Holmberg, E. 1958, *Medd. Lunds. Obs.*, Ser. II, Nr. 136.
Hubble, E. 1926, *Ap. J.*, **64**, 321.
———. 1929, *Proc. Nat. Acad. Sci.*, **15**, 168.
———. 1934, *ibid.*, **79**, 8.
———. 1936, *ibid.*, **84**, 270.
———. 1953, *M.N.R.A.S.*, **113**, 658.
Hubble, E., and Humason, M. L. 1931, *Ap. J.*, **74**, 43.
Humason, M. L. 1931, *Ap. J.*, **74**, 35.
———. 1936, *ibid.*, **83**, 10.
Humason, M. L., Mayall, N. U., and Sandage, A. R. 1956, *A.J.*, **61**, 97 (HMS).
Kristian, J., and Sachs, R. K. 1966, *Ap. J.*, **143**, 379.
McClure, R. D., and Crawford, D. L. 1971, *A.J.*, **76**, 31.

McNamara, P. H., and Langford, W. R. 1969, *Pub. A.S.P.*, **81**, 141.
McVittie, G. C. 1972, *M.N.R.A.S.*, **155**, 425.
Mathewson, D. S., and Ford, V. L. 1970, *Mem. R.A.S.*, **74**, 139.
Matthews, T. A., Morgan, W. W., and Schmidt, M. 1964, *Ap. J.*, **140**, 35.
Mattig, W. 1958, *Astr. Nach.*, **284**, 109.
Mayall, N. U., and Vaucouleurs, A. de. 1962, *A.J.*, **67**, 363.
Minkowski, R. 1960, *Ap. J.*, **132**, 908.
———. 1961, *A.J.*, **66**, 558.
Morgan, W. W., and Lesh, J. R. 1965, *Ap. J.*, **142**, 1364.
Noonan, T. W. 1971*a*, *A.J.*, **76**, 190.
———. 1971*b*, *Pub. A.S.P.*, **83**, 31.
Oke, J. B. 1971, *Ap. J.*, **170**, 193.
Oke, J. B., and Sandage, A. 1968, *Ap. J.*, **154**, 21.
Peach, J. V. 1969, *Nature*, **223**, 1140.
———. 1970, *Ap. J.*, **159**, 753.
Peebles, P. J. E. 1968, *Ap. J.*, **153**, 13.
———. 1969, *Nature*, **224**, 1093.
Peterson, B. A. 1970*a*, *A.J.*, **75**, 695.
———. 1970*b*, *Ap. J.*, **159**, 333.
———. 1970*c*, *Nature*, **227**, 54.
Pettit, E. 1954, *Ap. J.*, **120**, 413.
Philip, A. G. D., and Tifft, L. E. 1971, *A.J.*, **76**, 567.
Refsdal, S., Stabell, R., and de Lange, F. G. 1967, *Mem. R.A.S.*, **71**, 143.
Robertson, H. P. 1928, *Phil. Mag.*, **5**, 385.
Sandage, A. 1961*a*, *Ap. J.*, **133**, 355.
———. 1961*b*, *ibid.*, **134**, 916.
———. 1964, *Observatory*, **84**, 245.
———. 1968*a*, *Ap. J.* (*Letters*), **152**, L149.
———. 1968*b*, *Highlights in Astronomy*, *ed.* L. Perek (Dordrecht: D. Reidel Publishing Co.), p. 45.
———. 1968*c*, *Observatory*, **88**, 91.
———. 1969, *Ap. J.*, **157**, 515.
———. 1970*a*, *ibid.*, **162**, 841.
———. 1970*b*, *Physics Today*, **23** (No. 2), 44.
———. 1972*a*, *Ap. J.*, **173**, 485 (Paper I).
———. 1972*b*, *ibid.*, **176**, 21.
———. 1972*c*, *ibid.*, **178**, 25 (Paper III).
Schild, R., and Oke, J. B. 1971, *Ap. J.*, **169**, 209.
Scott, E. L. 1957, *A.J.*, **62**, 248.
Sersic, J. L. 1961, *Zs. f. Ap.*, **51**, 64.
Shane, C. D., and Wirtanen, C. A. 1954, *A.J.*, **59**, 285.
———. 1967, *Lick Obs. Bull.*, **22**, 1.
Shapiro, S. L. 1971, *A.J.*, **76**, 291.
Solheim, J. E., and Tinsley, B. M. 1972, in *External Galaxies and Quasi-stellar Objects, I.A.U. Symposium 44*, p. 397.
Spinrad, H., and Taylor, B. J. 1971, *Ap. J. Supp.*, **22**, 445.
Stebbins, J., and Whitford, A. E. 1948, *Ap. J.*, **108**, 413.
Tammann, G. A. 1972, *Astron. and Ap.*, in press.
Tinsley, B. M. 1968, *Ap. J.*, **151**, 547.
———. 1972, *Ap. J.* (*Letters*), **173**, L93.
Tinsley, B. M., and Spinrad, H. 1971, *Ap. and Space Sci.*, **12**, 118.
Vaucouleurs, G. de. 1961*a*, *Ap. J. Suppl.*, **5**, 233.
———. 1961*b*, *ibid.*, **6**, 213.
Vaucouleurs, G. de, and Malik, G. M. 1969, *M.N.R.A.S.*, **142**, 387.
Vignato, A., and Marcucci, R. 1971, *Ap. and Space Sci.*, **12**, 456.
Westerlund, B. E., and Smith, L. F. 1966, *Australian J. Phys.*, **19**, 181.
Westerlund, B. E., and Wall, J. V. 1969, *A.J.*, **74**, 335 (WW).
Whitford, A. E. 1971, *Ap. J.*, **169**, 215.